Heliyon 9 (2023) e17920

Contents lists available at ScienceDirect

Heliyon

journal homepage: www.cell.com/heliyon

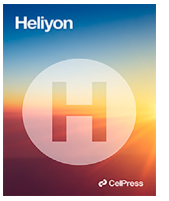

Research article

Computations for efficient thermal performance of Go + AA7072 with engine oil based hybrid nanofluid transportation across a Riga wedge ☆

Asmat Ullah Yahya [a], Sayed M Eldin [b], Suleman H Alfalqui [c], Rifaqat Ali [c], Nadeem Salamat [a], Imran Siddique [d,*], Sohaib Abdal [a,e]

[a] Department of Mathematics, Khwaja Fareed University of Engineering and Information Technology, Rahim Yar Khan, Pakistan
[b] Center of Research, Faculty of Engineering, Future University in Egypt, New Cairo 11835, Egypt
[c] Department of Mathematics, College of Science and Arts, King Khalid University, Muhayil 61413, Abha, Saudi Arabia
[d] Department of Mathematics, University of Management and Technology, Lahore 54770, Pakistan
[e] School of Mathematics, Northwest University, No.229 North Taibai Avenue, Xi'an 7100069, China

ARTICLE INFO

MSC:
00-01
99-00

Keywords:
Riga wedge
Magnetohydrodynamic
Hybrid nanofluid
Heat source
Williamson fluid
Runge-Kutta method

ABSTRACT

The demand for efficient heat transportation for the reliable functioning of mechanical processes is rising. The hybrid nanofluid emulsion is a related new concept in this research field. This communication pertains to mass and thermal transportation of Graphene oxide $(Go) + AA7072$ to be dissolved homogeneously in the bulk engine oil. In order to demonstrate the effectiveness of this hybrid nanofluid, a simple nanofluid Go/engine oil is also discussed. The flow of fluids occurs due to stretch in the wedge adjusted with Riga surface. The design of a hybrid nanofluid manifests the novelty of the work. The system of partial differential equations that are based on conservation principles of energy, momentum, and mass are transmuted to ordinary differential form. Numerical simulation is carried out on the Matlab platform by employing the Runge-Kutta approach along with a shooting tool. The influential parameters are varied to disclose the nature of physical quantities. The flow is accelerated with higher attributes of the modified Hartmann number, but it decelerates against the Weinberg number. The fluid's temperature rises with increment, in the concentration of nano-entities. The velocity for hybrid nanofluids is slower than that of mono nanofluids and the temperature distribution for hybrid nanofluids is greater than that of mono nanofluids. The fluid temperature increases with the concentration ϕ_2 of $AA7072$.

1. Introduction

During the previous few decades, numerous researchers are engaged to accomplish exceptional advancement in heat transportation, hence some new sorts of fluids are characterized, specifically nanofluids. These are advantageous to the thermal design of microelectronics, refrigeration and cooling, processors of PCs, portable, and so forth. Fundamentally, heat transfer relies on heat conductivity and molecule fixations of volume. At first Choi [1] reported that warmth moving paces in nanofluids were more note-

☆ Fully documented templates are available in the elsarticle package on CTAN.

* Corresponding author.
E-mail address: imransmsrazi@gmail.com (I. Siddique).

https://doi.org/10.1016/j.heliyon.2023.e17920
Received 17 October 2022; Received in revised form 1 July 2023; Accepted 1 July 2023

Available online 5 July 2023

Nomenclature

Latin Symbols

u, v	velocity components
(x, y)	Cartesian coordinates
U_w	velocity of the wall
k^*	permeability of porous medium
h_f	coefficient of heat transfer
T	temperature of nanoparticles
k	thermal conductivity
k_{nf}	nanofluid thermal conductivity
k_{hnf}	hybrid nanofluid thermal conductivity
ρC_p	heat capacity
J_0	electrodes current density
d	width of electrodes
M_0	magnate magnitization
U_e	free stream velocity
T_∞	ambient temperature
Q_0	heat source/sink coefficient
Mh	Hartmann number
K	porosity parameter
Pr	Prandtl number
Q	heat source
Ec	Eckert number
T_w	wall constant temperature
W_e	Weissenberg number
f	dimensionless streem function
B_i	Biot number
C_f	Skin friction coefficient
Nu	Nusselt number
Re_x	Local Reynolds number

Greek Symbols

μ	viscosity
μ_{nf}	viscosity of nanofluid
μ_{hnf}	hybrid nanofluid viscosity
ν	kinematic viscosity
σ	electrical conductivity
ρ	Density
ρ_{nf}	nanofluid density
ρ_{hnf}	hybrid nanofluid density
η	similarity variable
θ	similarity temperature
Γ	fluid relaxation time

Subscripts

p	nanoparticles
w	on the sheet surface
nf	nanofluid
hnf	hybrid nanofluid

worthy as compared to simple liquids. Gangadhar et al. [2,3] investigated impact of living microorganisms and nonlinear radiations on Oldroyd-B nanofluid flow. Ramana et al. [4] elaborated effect of Cattaneo-Christov heat flux theory on Oldroyd-B fluid past non-linear stretched flow. Gangadhar et al. [5] analyzed effect of convective heating on EMHD flow of radiative second-grade nanofluid across a Riga plate. Rao et al. [6] investigated spectral relaxation method for 3D MHD nanofluid flow across an elastic sheet due to convective heating. Gangadhar et al. [7,8] examined micropolar nanofluid flow over an elastic sheet with Newtonian heating. Gangadhar et al. [9] discussed nonlinear radiation case for Casson-Maxwell nanofluid flow along with chemical reactions. Gupta et al. [10] numerically investigate the radiative nanofluids with Marangoni convection. Kumar et al. [11] investigated the slip effects on nanofluid flow with melting phenomena. Gangadhar et al. [12] explained magnetization for burgers' fluid based on convective heating and heterogeneous-homogeneous reactions. Gangadhar et al. [13] analyzed effect of entropy depreciation on magnetized Boussinesq couple stress fluid with unstable heat production. Elangovan et al. [14] elaborated impact of entropy minimization on variable viscous couple stress fluid flow across a medium with thermal radiation and heat source/sink. Gangadhar et al. [15,16] investigated biconvective flow of magnetized couple stress fluid and for nanofluid by using different geometries. Many researchers were done similar work [17–20].

In recent times, scientists are planning hybrid nano-particles to enhance the heat transition rate of simple liquids/gases. The hybrid nano-particles are composed by blending materials of different kinds having nano-meter sized. The alloy of nano-particles is named hybrid nano-fluids. These fluids are utilized in many areas of daily life such as cooling in electronic networks, machine coolant, cooling vehicle motors, and so forth. Babazadeh et al. [21] scrutinized the behavior of Hybrid nanofluids in a permeable cavity with radiation effects. The comparative study of rotating surface of a disk and cone when Hybrid nanofluid flows between the canonical gap was deliberated by Gul et al. [22]. El-Gazar et al. [23] studied Fragmentary displaying for upgrading the thermal performance of conventional sunlight based as yet utilizing hybrid nanofluid. Raju et al. [24] examined the advancement in stream as well as the magnetohydrodynamic, radiative Newtonian fluid's thermal transit aspect with water base fluid and Al2O3+graphene hybrid nanofluid is hybrid nanofluid. The investigation of water-ethylene glycol streaming across a level chamber, consisting of hybrid nano-particles was broke down by Alwawi et al. [25]. The impacts of entropy creation on the MHD bounding layer stream of a mixture nanofluid of non-uniform viscous close to the lower stagnant locale of the heat circle was analyzed by Sakinder et al. [26]. Nanoparticles of all sorts, including Al_2O_3, Fe_3O_4, TiO_2 as well as CuO along with their base liquids like water, lubricating oils, glycol as well as ethylene glycol was scrutinized by Bashirnezhad et al. [27]. Mansoury et al. [28] depicted an extensive experimental analysis to assess the implication of nanoparticles on the efficiency of varied parallel stream thermal exchangers with similar heat transition exterior areas. Dadheech et al. [29,30] used different type of nanoparticles mixed in base fluid flowing over an inclined magnetic field. Agrawal et al. [31] discussed radiative impact on hybrid-nanofluids flow over a sponge medium. Elangovan et al. [32] discussed solution for radioactive MHD TiO2–Fe3O4/H2O nanofluid and its biological applications. Similar work was done by many researchers [33–35].

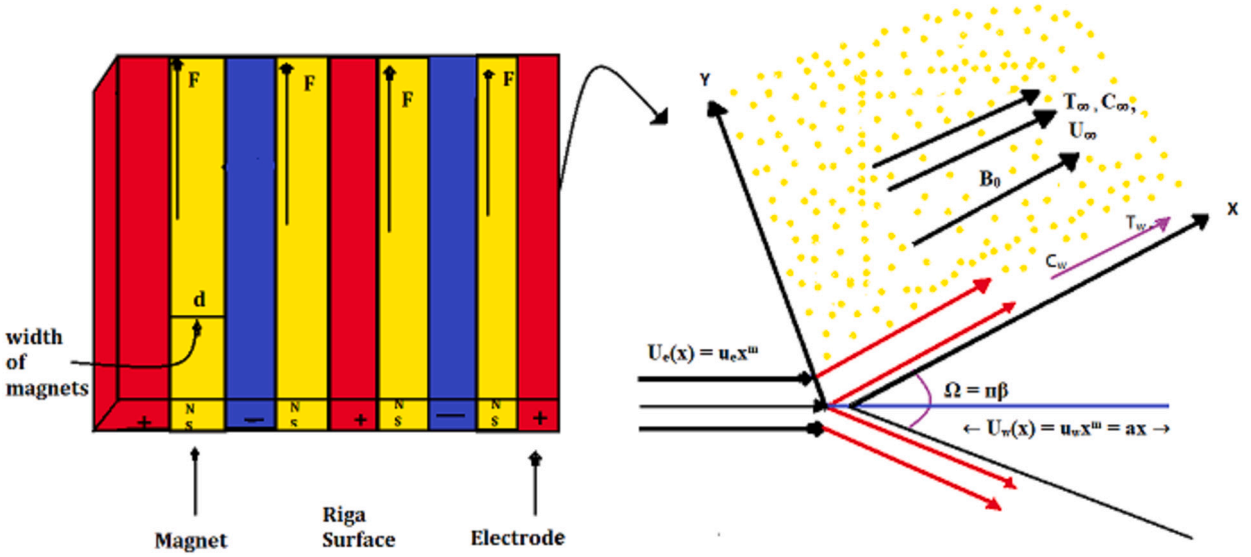

Fig. 1. Flowchart.

The property of liquids that do not submit to the laws of Newton is named non-Newtonian fluids. Many of the examples are seen in our daily life such as squeezed fruits, cleaner, dissolved margarine and ketchup, etc. Perhaps Williamson fluid is among the most important Non-Newtonian fluids was investigated by Williamson in 1929 [36]. Li et al. [37] scrutinized the motion of Williamson nanofluid, heat and mas transition through a permeable straining sheet. The numerical investigation of MHD and heat transit flow was examined by Qureshi et al. [38]. Yahya et al. [39] investigate the heat attributes of Williamson hybrid nanofluids through stretch surface with utilizing the engine oil as a base fluid. The study of Ag-Cu/EO across a stretched sheet having shape factor was deliberated by Jamshed et al. [40]. The study of outcomes of chemical reactions on Darcy Forcheimer Williamson nanofluid through a stretched linear sheet was examined by Rasool et al. [41]. Similar work on different non-Newtonian fluid were done by [42–46].

The stream with the effects of attractive field gives valuable outputs to design and mechanical procedures, for example, electrochemical miniature, atomic blenders, siphons, blood-stream estimation, and electromagnetic mixing in the projects of power and plasma control. Electromagnetic body power (Lorentz force) can handle the progressions of electrically leading liquids. In poor electrical conductive liquids, the Lorentz force is wasteful in light of the fact that it creates almost no flow. To defeat the weaknesses, Gailitis and Lielausis [47] demonstrated a gadget called Riga surface. Madhukesh et al. [48] investigated the flow of water containing SWCNT nanoparticles as well as floating microbes with a Riga surface. The study of non-Fourier heat flux, gyrotactic micro-organisms and double chemical reaction along the stream of rotating nanoparticles through Riga plate was analyzed by Ali et al. [49]. Rasool et al. [50] studied the generation of Lorentz force by Riga plate in the presence of Casson nanofluid with marangoni force. The theory of Cattaneo-Christove heat flow with activation energy and the flow of twisting Maxwell nanofluid across a Riga surface was discussed by Ali et al. [51].

The previous work has less consideration for the researchers because of the modern need. The necessities of modern civilization require efficient heat transportation to maintain thermal balance. An ongoing trend of problems in thermal engineering involve the study of hybrid nanofluid flow. In this scenario, a very rare emulsion of $AA7072$ + Graphene oxide/engine oil is considered to flow across a stretching wedge coupled with a Riga surface. To highlight the role of hybrid nanofluids, a comparative flow behavior of simple new fluid is also presented. The study of this manuscript motivates the researchers towards the hybridization of nanoparticles to enhance the significance of nanofluids which is beneficial in different fields as mentioned above. The parametric findings are evaluated numerically by coding the Runge-Kutta method in Matlab script. The results can be useful for the thermal performance of electronic equipment, and heat exchangers. Through this computational effort, we have successfully elucidated the parametric impacts on the dynamics of fluids.

2. Mathematical formulation of the problem

Consider a time-independent, incompressible, and two dimensional stream of hybrid nanofluids ($AA7072$/ Eigen oil) and ($AA7072 + GO$/ Eigen oil) over a Riga wedge as illustrated in Fig. 1. Let the $x - axis$ be parallel to the surface of the Riga wedge and also the $y - axis$ be perpendicular to it. The components of flow speed along the x and $y - axis$ are taken u and v, the dynamic viscosity of hybrid nano-liquid is μ_{hnf}, T is the temperature, ρ_{hnf} is the density of hybrid nanoparticles, k^* is the permeability of the porous medium, K_{hnf} is the hybrid nanofluid thermal conductivity, J_0 denotes the current density of electrodes, d is the width of electrodes, M_0 signifies the permanent magnates' magnetization, Γ is the fluid relaxation time, ρC_p is the heat capacity and Q_0 is the heat source/sink coefficient. In presence of above assumptions, the leading formation is given [39,52,53]:

Table 1
Physical characteristics of new species and base liquid.

Physical properties	AA_{7072}	GO	Engine oil
ρ (kg.m^{-3})	2720	1800	884
C_p (J(kg.°k	893	717	1910
κ (W(m.°k)	222	5000	0.144

Table 2
Physical characteristics of hybrid and single nanofluids [54–56].

Properties	Nanofluid	Hybrid Nanofluid
μ (viscosity)	$\mu_{nf} = \frac{\mu_f}{(1-\Phi)^{2.5}}$	$\mu_{hnf} = [\frac{\mu_f}{(1-\Phi_1)^{2.5}(1-\Phi_2)^{2.5}}]$
ρ (density)	$\rho_{nf} = \rho_f((1-\Phi)+\Phi\frac{\rho_s}{\rho_f}$	$\rho_{hnf} = [\rho_f(1-\Phi_2)((1-\Phi_1)+\Phi_1\frac{\rho_{s1}}{\rho_f})+\Phi_2\rho_{s2}]$
ρC_p (Heat capacity)	$(\rho C_p)nf = (\rho C_p)_f((1-\Phi)+\Phi\frac{(\rho C_p)_s}{(\rho C_p)_f}$	$(\rho C_p)_{hnf} = [(\rho C_p)_f(1-\Phi_2)((1-\Phi_1)+\Phi_1\frac{(\rho C_p)_{s1}}{(\rho C_p)_f})+\Phi_2(\rho C_p)_{s2}]$
κ (Thermal conductivity)	$\frac{\kappa_{nf}}{\kappa_f} = \frac{\kappa_s+(s_f-1)\kappa_f-(s_f-1)\Phi(\kappa_f-\kappa_s)}{\kappa_s+(s_f-1)\kappa_f+\Phi(\kappa_f-\kappa_s)}$	$\frac{\kappa_{hnf}}{\kappa_{bf}} = [\frac{\kappa_{s2}+(s_f-1)\kappa_{bf}-(s_f-1)\Phi_2(\kappa_{bf}-\kappa_{s2})}{\kappa_{s2}+(s_f-1)\kappa_{bf}+\Phi(\kappa_{bf}-\kappa_{s2})}]$ where $\frac{\kappa_{bf}}{\kappa_f} = [\frac{\kappa_{s1}+(s_f-1)\kappa_f-(s_f-1)\Phi_1(\kappa_f-\kappa_{s1})}{\kappa_{s1}+(s_f-1)\kappa_f+\Phi(\kappa_f-\kappa_{s1})}]$
σ (Electrical conductivity)	$\frac{\sigma_{nf}}{\sigma_f} = 1+\frac{3(\sigma-1)\Phi}{(\sigma+2)-(\sigma-1)\Phi}$	$\frac{\sigma_{hnf}}{\sigma_{bf}} = [1+\frac{3\Phi(\sigma_1\Phi_1+\sigma_2\Phi_2-\sigma_{bf}(\Phi_1+\Phi_2))}{(\sigma_1\Phi_1+\sigma_2\Phi_2+2\Phi\sigma_{bf})-\Phi\sigma_{bf}((\sigma_1\Phi_1+\sigma_2\Phi_2)-\sigma_{bf}(\Phi_1+\Phi_2))}]$

$$\frac{\partial u}{\partial x}+\frac{\partial v}{\partial y}=0, \tag{1}$$

$$u\frac{\partial u}{\partial x}+v\frac{\partial u}{\partial y}=\frac{\mu_{hnf}}{\rho_{hnf}}\frac{\partial^2 u}{\partial y^2}+\frac{\pi j_0 M_0}{8}-\frac{\mu_{hnf}}{\rho_{hnf}}\frac{u}{k^*}+\sqrt{2}\nu_f\Gamma\frac{\partial u}{\partial y}\frac{\partial^2 u}{\partial y^2}, \tag{2}$$

$$u\frac{\partial T}{\partial x}+v\frac{\partial T}{\partial y}=\frac{k_{hnf}}{(\rho C_p)_{hnf}}\frac{\partial^2 T}{\partial y^2}+\frac{\mu_{hnf}}{(\rho C_p)_{hnf}}(\frac{\partial u}{\partial x})^2+\frac{Q_0}{(\rho C_p)_{hnf}}(T-T_\infty). \tag{3}$$

The concerned boundary conditions (see equation (4)):

$$\left.\begin{aligned} u=U_w=ax, v=0, -k_{hnf}\frac{\partial T}{\partial y}=h_f(T-T_w),\ as\ y=0,\\ u\to U_e,\ T\to T_\infty,\ as\ y\to\infty. \end{aligned}\right\} \tag{4}$$

The wedge stretches nonlinearly with a velocity $U_w=u_w x^m$. The free stream velocity is denoted by $U_e=u_e x^m$, T_∞ is the ambient fluid temperature, h_f is the heat transfer coefficient and T_w is wall temperature. Here, Table 1 depicts the thermophysical properties. The volume distribution for $AA7072$ nanoparticles is 0.01 in bulk of GO / Engine oil is taken. In this model $\phi_1=0.04$ and $\phi_2=0$ for mono nanofluid GO / Engine oil. For hybrid nanofluid, volume fraction $\phi_1=0.03$ (GO) and $\phi_2=0.01$ $(AA7072)$ is considered. Thermo-physical attributes of hybrid nanofluid and nanofluids are disclosed in Table 2.

To redevelop the mathematical model (1)–(4), the similarity factors are stated. They are provided by (see [53]):

$$\eta=\sqrt{\frac{(m+1)U_e}{2x\nu}}y,\ U_e f'(\eta)=u,\ -\sqrt{\frac{(m+1)U_e\nu}{2x}}(f(\eta)+\frac{m-1}{m+1}\eta f'(\eta))=v,\ T=T_\infty+(T_w-T_\infty)\theta(\eta), \tag{5}$$

by using equation (5), the mass conservation eq. (1) is balanced and the eq. (2) to eq. (4) become:

$$(1+A_1 We f'')f'''-A_1(\beta f'^2-ff'')+A_1 M h exp(\alpha_h\eta)\frac{2}{m+1}-Kf'+\beta=0, \tag{6}$$

$$\theta''-\frac{k_f}{k_{hnf}}Pr(A_3 f\theta'-EcA_4 f''^2-Q\theta)=0, \tag{7}$$

$$\left.\begin{aligned} f(\eta)=0,\ f'(\eta)=0,\ \frac{k_{hnf}}{k_f}\theta'(\eta)=B_i(1-\theta(\eta)),\ at\ \eta=0,\\ f'(\infty)\to 1,\ \theta(\infty)\to 0,\ as\ \eta\to\infty. \end{aligned}\right\} \tag{8}$$

Equations (6)–(7) are the required ordinary differential equations and equation (8) is the required transformed boundary conditions. Where, $Mh=\frac{\pi J_0 M_0}{8a^2x^{2m-1}}$, $\alpha_h=(\frac{2\nu}{a(m+1)x^{m-1}})^{1/2}\frac{\pi}{d}$, $K=\frac{\mu}{k^*}$, $\beta=\frac{2m}{m+1}$, $Q=\frac{2Q_0}{a(\rho C_p)_{hnf}(m+1)x^{m+1}}$, $Ec=\frac{a^2x^{2m}}{(C_p)_f(T_w-T_\infty)}$, $Pr=\frac{\nu_f(\rho C_p)_f}{\kappa_f}$ and $We=\Gamma\frac{a^{3/2}(m+1)x^{(3m-1)/2}}{\nu^{1/2}}$ signify modified Hartmann number, non-dimensional parameter, porosity factor, wedge angle factor, heat generation factor, Eckert number, Prandtl number as well as Weissenberg number. The quantities of engineering significance (see [52,53]):

$$C_f=\frac{\tau_w}{\rho_f U_w^2},\ Nu=\frac{xq_w}{k_f(T_w-T_\infty)},\ \tau_w=\mu_{hnf}(\frac{\partial u}{\partial y}+\frac{\Gamma}{\sqrt{2}}(\frac{\partial u}{\partial y})^2),\ q_w=k_{hnf}\frac{\partial T}{\partial y},\ at\ y=0. \tag{9}$$

In transformed form equation (9) is transmuted into equation (10) by using equation (5):

Table 3
Comparison of $-\theta'(0)$ outcomes.

Pr	Wang. [57]	Khan and Pop [58]	Yahya et al. [39]	Our results
2.0	0.9114	0.9113	0.9112	0.9111
6.13	–	–	1.7597	1.7594
2.0	1.8954	1.8954	1.8953	1.8952
20.0	3.3539	3.3539	3.3540	3.3540

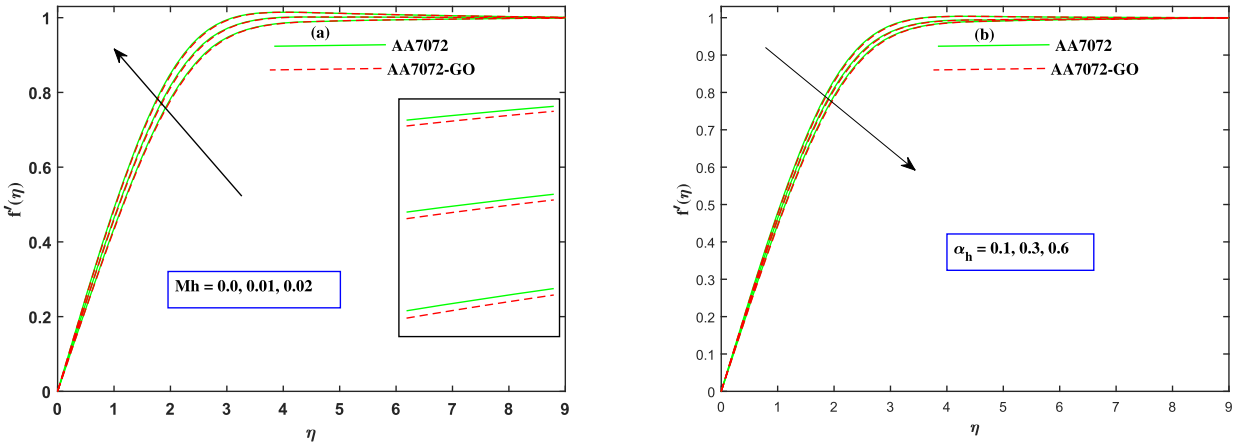

Fig. 2. Velocity $f'(\eta)$ fluctuation with (a) Mh and (b) α_h.

$$\begin{cases} Cf_x Re_x{}^{1/2} = \dfrac{f''(0) + We f''(0)^2}{A_4}, \\ Nu_x Re_x{}^{-1/2} = -\dfrac{\left[k_{hnf}\theta'(0)\right]}{k_f}. \end{cases} \tag{10}$$

3. Solution procedure

For the computation of results, the numerical solution procedure of equation (1) to equation (3) is desired as it is very difficult to attain an analytical solution. As a result, the Runge-Kutta numerical algorithm is employed to estimate the given model. The strategy's fundamental design is to transform derivatives of high order into order first derivatives as given below:

$s_1' = s_2$
$s_2' = s_3$
$(1 + We A_1 s_3)s_3' = A_1(s_2^2 - s_1 s_3) - A_1 M_h exp(\alpha_h \eta)\frac{2}{m+1} + K_p s_2 - \beta$
$s_4' = s_5$
$s_5' = \frac{k_f}{k_{hnf}} Pr(A_3 s_1 s_5 - Ec A_4 s_3^2 - Q s_4)$
along with the boundary conditions:
$s_1 = 0,\ s_2 = 0,\ \frac{k_{hnf}}{k_f} s_5 = B_i(1 - s_4)$, at $\eta = 0$
$s_2 \to 0,\ s_4 \to 0$ as $\eta \to \infty$.

4. Discuss on results

Here, the results are computed and presented for numerical solutions for two cases, case-i = $AA7072$ / Engine oil and case-ii = $AA7072 + GO$ / Engine oil. The reliability of the arithmetical strategy is determined in limiting situations, as revealed in Table 3.

For numerous parameters graphical findings the range of the prominent parameters are $0 \le Mh \le 0.02$, $0.1 \le \alpha_h \le 0.6$, $0.1 \le We \le 2.0$, $0.1 \le K_p \le 2.0$, $0.1 \le m \le 2.0$, $0.1 \le \beta \le 1.0$, $0.1 \le Ec \le 0.3$, $0.01 \le Q \le 0.1$, and $0.5 \le B_i \le 1.5$. When the dimensionless number of impacts is changed in adequate variations, calculations are made to elaborate the heat and mass transition by Williamson hybrid nanofluid. Figs. 2 through 5 show the findings for $AA7072$ /Engine oil and $AA7072 + GO$ /Engine oil. The specified values of the Prandtl number $Pr = 30$ are used here. The impacts of modified Hartmann number M_h and non-dimensional factor α_h on velocity component $f'(\eta)$ are illustrated in Fig. 2. It is encountered that the flow of both nanofluids intensifies with raising M_h and diminishes with growing α_h. The modified Hartmann number M_h is linked to the Riga exterior layout, that minimizes friction in the stream and thus results in acceleration. Fig. 3 portrays the implication of the Weissenberg number We and the porous medium K_p on $f'(\eta)$. The motion slows as it approaches (We and K_p). The main cause for the velocity reductions is that We are the ratio of the

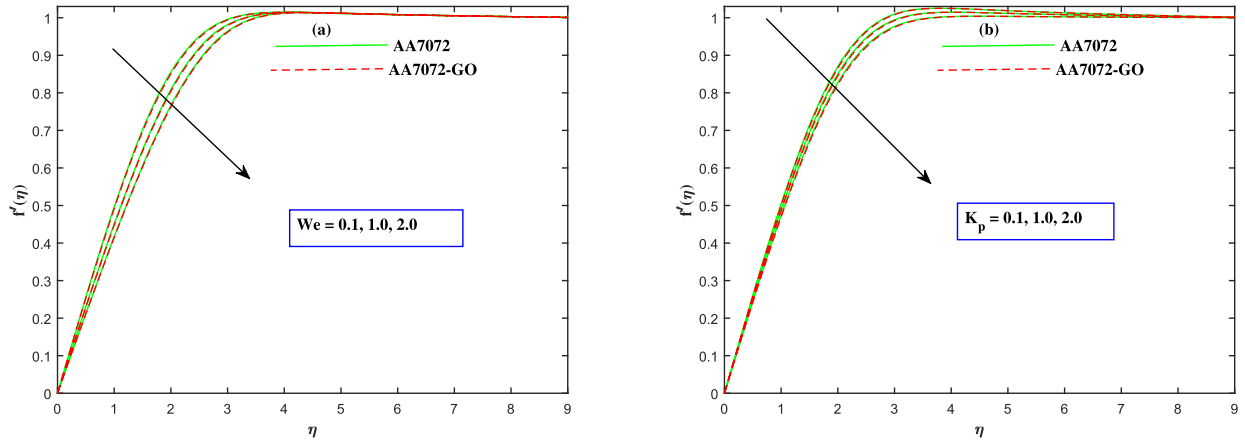

Fig. 3. Velocity $f'(\eta)$ fluctuation with (a) We and (b) K_p.

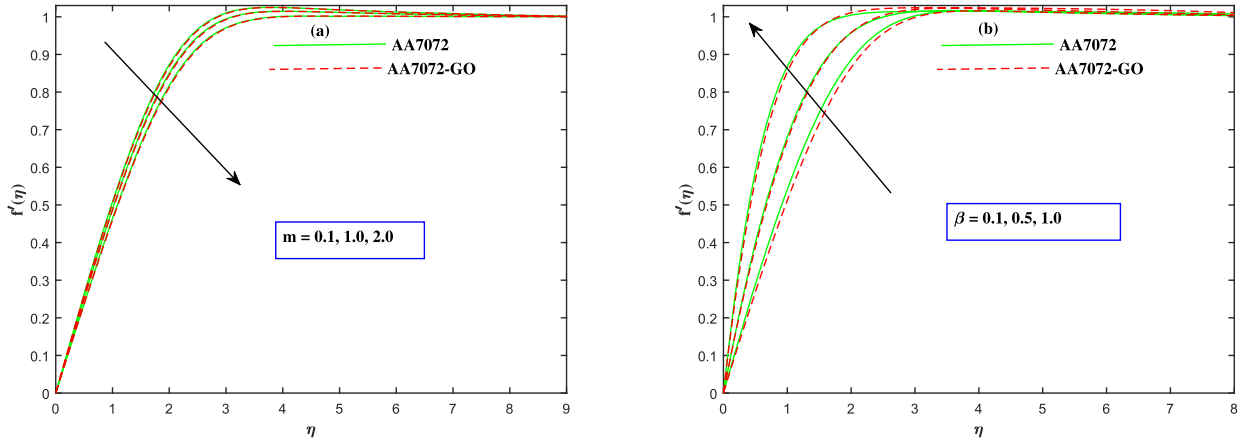

Fig. 4. Velocity $f'(\eta)$ fluctuation with (a) m and (b) β.

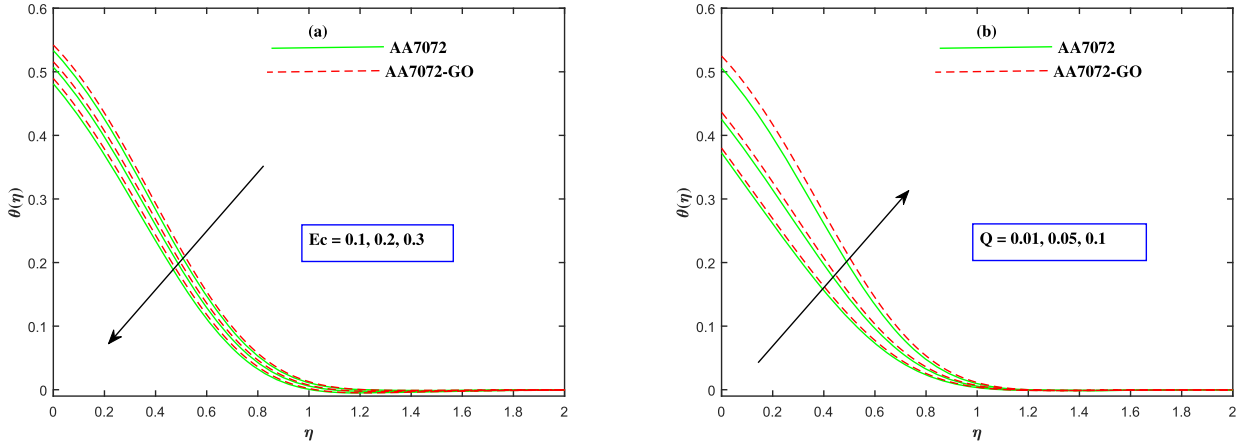

Fig. 5. Temperature $\theta(\eta)$ fluctuation with (a) Ec and (b) Q.

specific relaxation time. When K_p improves, there is more strong opposition in the stream, so velocity declines. Fig. 4 illustrates the consequences of the nonlinear factor m as well as the Wedge angle β on the flow rate $f'(\eta)$. The velocity lessens as the factor m raises, but it expands quite faster as β intensifies. Fig. 5 depicts the thermal gradient for simple as well as hybrid nanofluids for distinct attributes of Ec and Q. It can be observed that as Ec grows, the temperature of both liquids lowers. The main motive for this delay would be that higher values of Ec transform mechanical power to heat energy via thermal dissipation. Temperature, the other side,

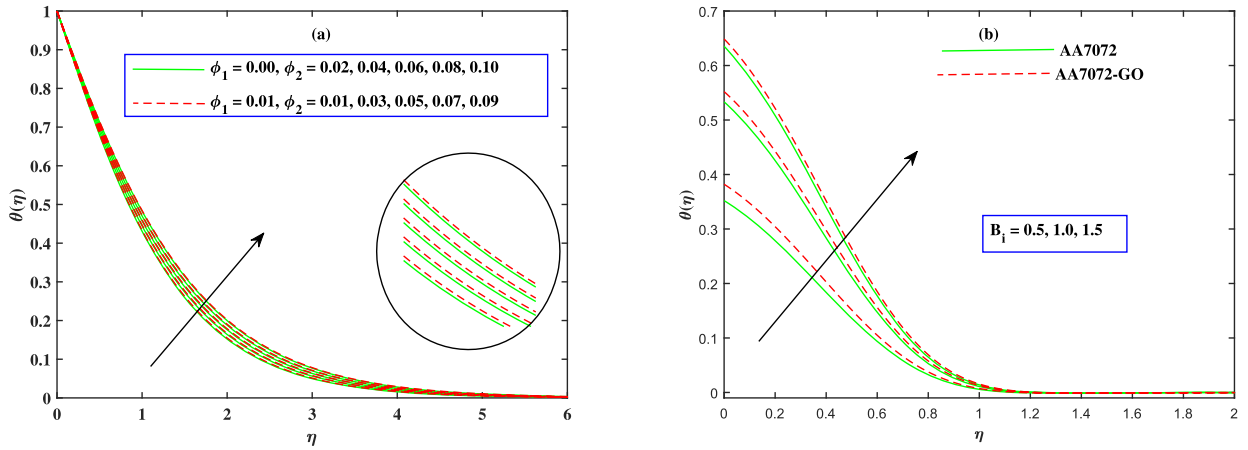

Fig. 6. Temperature $\theta(\eta)$ fluctuation with (a) Φ and (b) B_i.

Table 4
Outcomes for Skin friction factor $-f''(0)$.

We	β	K_p	Mh	m	α_h	$AA7072$	$AA7072+Go$	Total CPU Time ($AA7072$)	Total CPU Time ($AA7072+Go$)
0.1	0.01	1.0	0.02	0.5	0.01	0.5811	0.5753	14.620497	14.504887
0.2						0.5727	0.5671	14.691500	14.650395
0.3						0.5648	0.5595	14.500567	15.075104
0.1	0.01					0.5727	0.5671	14.869099	14.535016
	0.02					0.5881	0.5829	14.622750	14.589662
	0.03					0.6034	0.5986	14.243131	14.438235
	0.01	0.1				0.5904	0.5849	14.747698	14.243213
		0.5				0.5825	0.5770	14.498096	14.328429
		1.0				0.5727	0.5671	14.731030	14.453568
		1.0	0.01			0.5357	0.5306	14.820237	10.815037
			0.02			0.5727	0.5671	14.619012	14.417475
			0.03			0.6086	0.6026	14.831071	15.022862
			0.02	0.1		0.5989	0.5930	14.956907	14.763952
				0.3		0.5838	0.5781	14.668503	14.830897
				0.5		0.5727	0.5671	14.734096	15.152299
				0.5	0.01	0.5727	0.5671	15.391032	15.755734
					0.02	0.5709	0.5653	15.184299	15.390768
					0.03	0.5691	0.5663	14.213779	14.311109

Table 5
Outcomes for Nusselt number $-\theta'(0)$.

Ec	Q	B_i	$AA7072$	$AA7072+Go$
0.01	0.1	1.0	0.4667	0.4606
0.02			0.4926	0.4869
0.03			0.5190	0.5132
	0.01		0.6274	0.6256
	0.05		0.5748	0.5719
	0.1		0.4667	0.4606
	0.1	0.5	0.3246	0.3211
		1.0	0.4667	0.4606
		1.5	0.5740	0.5385

rises with expanding Q values for both liquids. Physically, it generates heat from the surface due to $T_w > T_\infty$, which increases the temperature. Fig. 6 depicts the consequences of volume fractions ϕ_2 as well as B_i. It can be seen as the valuation of ϕ_2 accumulates, so does the temperature. The basic explanation for this phenomenon is that as ϕ_2 grows, so does heat conductivity. Temperature improves the Biot number including both fluids. Biot number and temperature have a direct physical correlation. As an outcome, as the worth of B_i grows, consequently the temperature. Furthermore, the outcomes of skin friction $-f''(0)$ for the varied inputs of the quantities We, β, K_p, M_h, m as well as α_h are displayed in Table 4. Absolute values of $-f''(0)$ are noticed to be boosted by M_h and β. Whenever the parameters We, K_p, m, and α_h are elevated, the valuation of $-f''(0)$ reduces. In addition, the Nusselt number $-\theta'(0)$ is improved by improving values of Ec and B_i, as depicted in Table 5. It is ascertained that $-\theta'(0)$ lowers in regards to the heat source factor Q.

5. Conclusions

A theoretical description of heat and mass transport of hybrid nanofluid $(AA7072+Go)$/engine oil due to an extending Riga wedge is presented in this paper. Numerical findings are computed with varying inputs of pertinent factors like modified Hartmann number (M_h), Weisnberg number (We) dimensionless parameter (α_h), wedge angle factor (β), heat source factor (Q), Eckert number (Ec), Biot number (B_i), volume fraction (ϕ_2), suction parameter (K_p) and nonlinear stretching parameter (m). The following outcomes are yielded:

- Velocity profile $f'(\eta)$ increases when modified Hartmann number M_h takes higher inputs.
- Velocity profile $f'(\eta)$ decreases with the rising values of α_h, K_p, We, and m while it upsurges with the rising values of β.
- Temperature $\theta(\eta)$ decreases when the values of Ec intensified. On the other hand, temperature increases rapidly when Q increases.
- The hybrid nanofluid temperature increases with concentration ϕ_2.
- The temperature of fluid also increases with the Biot number.
- Skin friction factor decreases with the rising values of α_h, K_p, We, and m for both fluids ($i = AA7072$, $ii = AA7072 + GO$)
- On the other hand, increases for β and M_h.
- Nusselt number $-\theta'(0)$ increases for B_i and Q while decreases for Eckert number Ec in both cases.

Future direction

This study may be extended for Maxwell nanofluid, Oldroyd-B nanofluid, tangent hyperbolic and viscoelastic Jeffery nanofluid for different geometries.

CRediT authorship contribution statement

Asmat Ullah Yahya: Analyzed and interpreted the data; Wrote the paper.
Sayed M Eldin: Conceived and designed the analysis; Wrote the paper.
Suleman H Alfalqui: Conceived and designed the analysis; Contributed analysis tools or data.
Rifaqat Ali, Nadeem Salamat: Analyzed and interpreted the data; Contributed analysis tools or data.
Imran Siddique, Sohaib Abdal: Conceived and designed the analysis; Analyzed and interpreted the data.

Declaration of competing interest

The authors declare that they have no known competing financial interests or personal relationships that could have appeared to influence the work reported in this paper.

Data availability

Data will be made available on request.

Acknowledgement

The authors extend their appreciation to the Deanship of Scientific Research at King Khalid University Saudi Arabia for funding this work through large group Research Project under grant number RGP 2/554/44.

References

[1] S.U. Choi, J.A. Eastman, Enhancing thermal conductivity of fluids with nanoparticles, Tech. Rep., Argonne National Lab., IL (United States), 1995.
[2] K. Gangadhar, M.A. Kumari, M. Venkata Subba Rao, A.J. Chamkha, Oldroyd-B nanoliquid flow through a triple stratified medium submerged with gyrotactic bioconvection and nonlinear radiations, Arab. J. Sci. Eng. (2022) 1–13.
[3] K. Gangadhar, K. Bhanu Lakshmi, T. Kannan, A.J. Chamkha, Bioconvective magnetized oldroyd-B nanofluid flow in the presence of Joule heating with gyrotactic microorganisms, in: Waves in Random and Complex, Media, 2022, pp. 1–21.
[4] K. Venkata Ramana, K. Gangadhar, T. Kannan, A.J. Chamkha, Cattaneo–Christov heat flux theory on transverse MHD Oldroyd-B liquid over nonlinear stretched flow, J. Therm. Anal. Calorim. (2022) 1–11.
[5] K. Gangadhar, M.A. Kumari, A.J. Chamkha, EMHD flow of radiative second-grade nanofluid over a Riga plate due to convective heating: revised Buongiorno's nanofluid model, Arab. J. Sci. Eng. 47 (7) (2022) 8093–8103.
[6] M. Venkata Subba Rao, K. Gangadhar, P. Varma, A spectral relaxation method for three-dimensional MHD flow of nanofluid flow over an exponentially stretching sheet due to convective heating: an application to solar energy, Indian J. Phys. 92 (12) (2018) 1577–1588.
[7] K. Gangadhar, T. Kannan, P. Jayalakshmi, Magnetohydrodynamic micropolar nanofluid past a permeable stretching/shrinking sheet with Newtonian heating, J. Braz. Soc. Mech. Sci. Eng. 39 (11) (2017) 4379–4391.
[8] K. Gangadhar, M. Prameela, A.J. Chamkha, Thermally radiated micro-polar fluid with space-dependent heat source: modified Cattaneo-Christov heat flux theory, Proc. Inst. Mech. Eng., E J. Process Mech. Eng. (2022) 09544089221131679.
[9] K. Gangadhar, E. Mary Victoria, K. Bhanu Lakshmi, A.J. Chamkha, Nonlinear radiation phenomena for Casson–Maxwell nanoliquid flow with chemical reactions, Proc. Inst. Mech. Eng., E J. Process Mech. Eng. (2022) 09544089221132356.

[10] R. Gupta, M. Gaur, Q. Al-Mdallal, S.D. Purohit, D.L. Suthar, Numerical study of the flow of two radiative nanofluids with Marangoni convection embedded in porous medium, J. Nanomater. 2022 (2022) 1–7.
[11] N. Kumar, R.N. Jat, S. Sinha, P.K. Dadheech, P. Agrawal, S.D. Purohit, K.S. Nisar, Radiation and slip effects on MHD point flow of nanofluid towards a stretching sheet with melting heat transfer, Heat Transf. 51 (4) (2022) 3018–3034.
[12] K. Gangadhar, M.A. Kumari, M.V. Subba Rao, K. Alnefaie, I. Khan, M. Andualem, Magnetization for Burgers' fluid subject to convective heating and heterogeneous-homogeneous reactions, Math. Probl. Eng. 2022 (2022) 1–15.
[13] K. Gangadhar, A.J. Chamkha, et al., Entropy minimization on magnetized Boussinesq couple stress fluid with non-uniform heat generation, Phys. Scr. 96 (9) (2021) 095205.
[14] K. Elangovan, K. Subbarao, K. Gangadhar, Entropy minimization for variable viscous couple stress fluid flow over a channel with thermal radiation and heat source/sink, J. Therm. Anal. Calorim. 147 (23) (2022) 13499–13507.
[15] K. Gangadhar, P. Manasa Seshakumari, M. Venkata Subba Rao, A.J. Chamkha, Biconvective transport of magnetized couple stress fluid over a radiative paraboloid of revolution, Proc. Inst. Mech. Eng., E J. Process Mech. Eng. 236 (4) (2022) 1661–1670.
[16] K. Gangadhar, K.B. Lakshmi, T. Kannan, A.J. Chamkha, Stefan blowing on chemically reactive nano-fluid flow containing gyrotactic microorganisms with leading edge accretion (or) ablation and thermal radiation, Indian J. Phys. (2021) 1–14.
[17] L. Ali, B. Ali, M.B. Ghori, Melting effect on Cattaneo–Christov and thermal radiation features for aligned MHD nanofluid flow comprising microorganisms to leading edge: FEM approach, Comput. Math. Appl. 109 (2022) 260–269.
[18] S. Abdal, I. Siddique, A. Ahmadian, S. Salahshour, M. Salimi, Enhanced heat transportation for bioconvective motion of Maxwell nanofluids over a stretching sheet with Cattaneo–Christov flux, Mech. Time-Depend. Mater. (2022) 1–16.
[19] L. Ali, B. Ali, X. Liu, S. Ahmed, M.A. Shah, Analysis of bio-convective MHD Blasius and Sakiadis flow with Cattaneo-Christov heat flux model and chemical reaction, Chin. J. Phys.
[20] S. Afzal, I. Siddique, F. Jarad, R. Ali, S. Abdal, S. Hussain, Significance of double diffusion for unsteady Carreau micropolar nanofluid transportation across an extending sheet with thermo-radiation and uniform heat source, Case Stud. Therm. Eng. 28 (2021) 101397.
[21] H. Babazadeh, Z. Shah, I. Ullah, P. Kumam, A. Shafee, Analysis of hybrid nanofluid behavior within a porous cavity including Lorentz forces and radiation impacts, J. Therm. Anal. Calorim. 143 (2) (2021) 1129–1137.
[22] T. Gul, M. Bilal, W. Alghamdi, M.I. Asjad, T. Abdeljawad, et al., Hybrid nanofluid flow within the conical gap between the cone and the surface of a rotating disk, Sci. Rep. 11 (1) (2021) 1–19.
[23] E. El-Gazar, W. Zahra, H. Hassan, S.I. Rabia, Fractional modeling for enhancing the thermal performance of conventional solar still using hybrid nanofluid: energy and exergy analysis, Desalination 503 (2021) 114847.
[24] C. Raju, S.M. Upadhya, D. Seth, Thermal convective conditions on MHD radiated flow with suspended hybrid nanoparticles, Microsyst. Technol. 27 (5) (2021) 1933–1942.
[25] F.A. Alwawi, M.Z. Swalmeh, A.S. Qazaq, R. Idris, Heat transmission reinforcers induced by MHD hybrid nanoparticles for water/water-EG flowing over a cylinder, Coatings 11 (6) (2021) 623.
[26] S. Sakinder, T. Salahuddin, F.S. Al-Mubaddel, M.M. Alam, I. Ahmad, Influence of entropy generation on hybrid nanoparticles near the lower region of solid sphere, Case Stud. Therm. Eng. 26 (2021) 101038.
[27] K. Bashirnezhad, M.M. Rashidi, Z. Yang, S. Bazri, W.-M. Yan, A comprehensive review of last experimental studies on thermal conductivity of nanofluids, J. Therm. Anal. Calorim. 122 (2) (2015) 863–884.
[28] D. Mansoury, F. Ilami Doshmanziari, S. Rezaie, M.M. Rashidi, Effect of Al2O3/water nanofluid on performance of parallel flow heat exchangers, J. Therm. Anal. Calorim. 135 (1) (2019) 625–643.
[29] P.K. Dadheech, P. Agrawal, A. Sharma, K.S. Nisar, S.D. Purohit, Marangoni convection flow of γ–Al2O3 nanofluids past a porous stretching surface with thermal radiation effect in the presence of an inclined magnetic field, Heat Transf. 51 (1) (2022) 534–550.
[30] P.K. Dadheech, P. Agrawal, A. Sharma, K.S. Nisar, S.D. Purohit, Transportation of Al2O3-SiO2-TiO2 modified nanofluid over an exponentially stretching surface with inclined magnetohydrodynamic, Therm. Sci. 25 (Spec. issue 2) (2021) 279–285.
[31] P. Agrawal, P.K. Dadheech, R. Jat, D. Baleanu, S.D. Purohit, Radiative MHD hybrid-nanofluids flow over a permeable stretching surface with heat source/sink embedded in porous medium, Int. J. Numer. Methods Heat Fluid Flow 31 (8) (2021) 2818–2840.
[32] K. Elangovan, K. Subbarao, K. Gangadhar, An analytical solution for radioactive MHD flow TiO2–Fe3O4/H2O nanofluid and its biological applications, Int. J. Ambient Energy 43 (1) (2022) 7576–7587.
[33] G. Xiang, X. Gao, W. Tang, X. Jie, X. Huang, Numerical study on transition structures of oblique detonations with expansion wave from finite-length cowl, Phys. Fluids 32 (5) (2020) 056108.
[34] M. Qu, T. Liang, J. Hou, Z. Liu, E. Yang, X. Liu, Laboratory study and field application of amphiphilic molybdenum disulfide nanosheets for enhanced oil recovery, J. Pet. Sci. Eng. 208 (2022) 109695.
[35] X. Fan, G. Wei, X. Lin, X. Wang, Z. Si, X. Zhang, Q. Shao, S. Mangin, E. Fullerton, L. Jiang, et al., Reversible switching of interlayer exchange coupling through atomically thin VO_2 via electronic state modulation, Matter 2 (6) (2020) 1582–1593.
[36] R.V. Williamson, The flow of pseudoplastic materials, Ind. Eng. Chem. 21 (11) (1929) 1108–1111.
[37] Y.-X. Li, M.H. Alshbool, Y.-P. Lv, I. Khan, M.R. Khan, A. Issakhov, Heat and mass transfer in MHD Williamson nanofluid flow over an exponentially porous stretching surface, Case Stud. Therm. Eng. 26 (2021) 100975.
[38] M. Amer Qureshi, Numerical simulation of heat transfer flow subject to MHD of Williamson nanofluid with thermal radiation, Symmetry 13 (1) (2021) 10.
[39] A.U. Yahya, N. Salamat, W.-H. Huang, I. Siddique, S. Abdal, S. Hussain, Thermal charactristics for the flow of Williamson hybrid nanofluid (MoS_2 + ZnO) based with engine oil over a streched sheet, Case Stud. Therm. Eng. 26 (2021) 101196.
[40] W. Jamshed, S.U. Devi, K.S. Nisar, Single phase based study of Ag-Cu/EO Williamson hybrid nanofluid flow over a stretching surface with shape factor, Phys. Scr. 96 (6) (2021) 065202.
[41] G. Rasool, T. Zhang, A.J. Chamkha, A. Shafiq, I. Tlili, G. Shahzadi, Entropy generation and consequences of binary chemical reaction on MHD Darcy–Forchheimer Williamson nanofluid flow over non-linearly stretching surface, Entropy 22 (1) (2020) 18.
[42] S. Abdal, I. Siddique, S. Afzal, S. Sharifi, M. Salimi, A. Ahmadian, An analysis for variable physical properties involved in the nano-biofilm transportation of Sutterby fluid across shrinking/stretching surface, Nanomaterials 12 (4) (2022) 599.
[43] B. Ali, I. Siddique, A. Shafiq, S. Abdal, I. Khan, A. Khan, Magnetohydrodynamic mass and heat transport over a stretching sheet in a rotating nanofluid with binary chemical reaction, non-fourier heat flux, and swimming microorganisms, Case Stud. Therm. Eng. 28 (2021) 101367.
[44] S. Abdal, I. Siddique, D. Alrowaili, Q. Al-Mdallal, S. Hussain, Exploring the magnetohydrodynamic stretched flow of Williamson Maxwell nanofluid through porous matrix over a permeated sheet with bioconvection and activation energy, Sci. Rep. 12 (1) (2022) 1–12.
[45] S. Abdal, U. Habib, I. Siddique, A. Akgül, B. Ali, Attribution of multi-slips and bioconvection for micropolar nanofluids transpiration through porous medium over an extending sheet with PST and PHF conditions, Int. J. Appl. Comput. Math. 7 (6) (2021) 1–21.
[46] U. Habib, S. Abdal, I. Siddique, R. Ali, A comparative study on micropolar, Williamson, Maxwell nanofluids flow due to a stretching surface in the presence of bioconvection, double diffusion and activation energy, Int. Commun. Heat Mass Transf. 127 (2021) 105551.
[47] A. Gailitis, On the possibility to reduce the hydrodynamic drag of a plate in an electrolyte, Appl. Magnetohydrodynamics, Rep. Inst. Phys. Riga 13 (1961) 143–146.

[48] J.K. Madhukesh, G.K. Ramesh, E.H. Aly, A.J. Chamkha, Dynamics of water conveying SWCNT nanoparticles and swimming microorganisms over a Riga plate subject to heat source/sink, Alex. Eng. J. 61 (3) (2022) 2418–2429.
[49] B. Ali, S.U. Devi, A.K. Hussein, S. Hussain, et al., Transient rotating nanofluid flow over a Riga plate with gyrotactic micro-organisms, binary chemical reaction and non-Fourier heat flux, Chin. J. Phys. 73 (2021) 732–745.
[50] G. Rasool, A. Shafiq, C.M. Khalique, Marangoni forced convective Casson type nanofluid flow in the presence of Lorentz force generated by Riga plate, Discrete Contin. Dyn. Syst., Ser. S 14 (7) (2021) 2517.
[51] B. Ali, P. Pattnaik, R.A. Naqvi, H. Waqas, S. Hussain, Brownian motion and thermophoresis effects on bioconvection of rotating Maxwell nanofluid over a Riga plate with arrhenius activation energy and Cattaneo-Christov heat flux theory, Therm. Sci. Eng. Prog. 23 (2021) 100863.
[52] T. Salahuddin, M. Khan, T. Saeed, M. Ibrahim, Y.-M. Chu, Induced MHD impact on exponentially varying viscosity of Williamson fluid flow with variable conductivity and diffusivity, Case Stud. Therm. Eng. 25 (2021) 100895.
[53] S.U. Devi, S.A. Devi, Heat transfer enhancement of cu- $al\_\{2\}o\_\{3\}$/water hybrid nanofluid flow over a stretching sheet, J. Niger. Math. Soc. 36 (2) (2017) 419–433.
[54] B. Ali, R.A. Naqvi, D. Hussain, O.M. Aldossary, S. Hussain, Magnetic rotating flow of a hybrid nano-materials Ag-MoS2 and Go-MoS2 in C2H6O2-H2O hybrid base fluid over an extending surface involving activation energy: FE simulation, Mathematics 8 (10) (2020) 1730.
[55] B. Ali, R.A. Naqvi, L. Ali, S. Abdal, S. Hussain, A comparative description on time-dependent rotating magnetic transport of a water base liquid H_2O with hybrid nano-materials Al_2O_3-Cu and Al_2O_3-TiO_2 over an extending sheet using Buongiorno model: finite element approach, Chin. J. Phys. 70 (2021) 125–139.
[56] A.U. Yahya, I. Siddique, F. Jarad, N. Salamat, S. Abdal, Y. Hamed, K.M. Abualnaja, S. Hussain, On the enhancement of thermal transport of Kerosene oil mixed TiO_2 and SiO_2 across Riga wedge, Case Stud. Therm. Eng. (2022) 102025.
[57] C. Wang, Free convection on a vertical stretching surface, J. Appl. Math. Mech./Z. Angew. Math. Mech. 69 (11) (1989) 418–420.
[58] W. Khan, I. Pop, Boundary-layer flow of a nanofluid past a stretching sheet, Int. J. Heat Mass Transf. 53 (11–12) (2010) 2477–2483.